© 1997 The Chemical Society of Japan

Bull. Chem. Soc. Jpn., ***70***, 777—787 (1997)

Comparative Ab initio and Hybrid DFT Studies Relevant to an Experimental Investigation of Neutral and Cationic [Si, P, H_2] Isomers

Jan Hrušák,* Detlef Schröder,† Helmut Schwarz,† and Suehiro Iwata††

Institute of Physical Chemistry, Academy of Sciences of the Czech Republic,
Dolejškova 3, CZ-182 23 Praha, Czech Republic

†Institut für Organische Chemie der Technischen Universität Berlin, Straße des 17. Juni 135, D-10623 Berlin, Germany

††Institute for Molecular Sciences, Myodaiji, 444 Okazaki

(Received November 26, 1996)

The neutral and the lowest cationic (singlet and triplet) potential-energy surfaces of [Si, P, H_2] have been explored by means of ab initio MO calculations at the G2 level of theory as well as the hybrid DFT (B3LYP/6-311G**) method. Contrary to the neutral and triplet surfaces, where the $H_2SiP^{+/0}$ isomers represent the global minima, for the singlet cation a doubly bridged $P(H)_2Si^+$ structure has been identified as the most stable isomer, with the non-bridged H_2SiP^+ species being significantly less stable ($\Delta E = 31.7$ kcal mol^{-1} at G2). As far as the comparison of the two quantum-chemical methods (i.e. G2 and B3LYP) is concerned, the calculated relative energies ΔE are quite close to each other, with deviations smaller than 4 kcal mol^{-1}. However, while the non-bridged $SiPH_2^+$ ($^1A'$) represents a minimum at the G2 level, it could not be located using the hybrid DFT method. The computationally predicted singlet and triplet [Si, P, H_2]$^+$ potential-energy surfaces provide insight into the course of the ion/molecule reactions of $Si^{+\bullet}$ with phosphine and P^+ with silane, respectively, which were examined experimentally. Thus, the reaction of the doublet species $Si^{+\bullet}$ with phosphine allows access to the non-classical, bridged $P(H)_2Si^+$ structure, while in the reaction of the P^+ triplet cation with silane, no evidence for Si–P bond formation is obtained.

Silicon-containing molecules have attracted considerable interest during the last two decades,[1,2] due to their relevance in technology, applied chemistry, and organic synthesis. In addition, neutral and cationic silicon compounds have been suggested to play an important role in interstellar chemistry.[3,4] The element silicon is quite abundant in inter- and circumstellar environments, and molecules such as SiC_n ($n = 1, 2, 4$), SiH_4, or SiN have been identified.[4c] Furthermore, from a conceptual point of view, the relationship between carbon and silicon occupies a unique position in understanding the different behavior of the elements Li–Ne as compared to the heavier main-group elements.[5]

In the last few years, gas-phase reactions of atomic $Si^{+\bullet}$ cations with a variety of molecules have been examined by different experimental and theoretical means,[6] as recently reviewed by Böhme as well as Goldberg and Schwarz.[7] However, most of these studies dealt with the interaction of silicon with the elements H–Ne, and elements of the higher periods have not been studied very much.[8] Among these investigations, a particularly exciting finding is the existence of bridged disilyne Si_2H_2 which has been predicted in many theoretical studies,[9—15] but only recently was confirmed experimentally.[16] Lischka and Kohler were the first to suggest,[10] based on SCF DZP calculations, that the most stable structure of disilyne corresponds to a doubly bridged, C_{2v}-symmetrical isomer. This bridged, non-classical structure of disilyne was later confirmed by correlated ab initio calculations, and nowadays no less than eleven different [Si_2, H_2] structures have been predicted to exist on the very flat potential energy surface (PES) of this particular system.[15]

Recently, we investigated some representatives of the series H_2SiX using the time-honored approach of combining theoretical calculations with advanced mass spectrometric techniques.[17,18] In this context, the existence of a doubly bridged cationic structure of $P(H)_2Si^+$ was predicted.[19] Meanwhile, Schoeller and Busch[20] examined [Si, P, H_2]$^+$ using MP2 and QCISD methods with DZP and 6-31+G** basis sets and found, among a few other structures, a singlet state with a doubly-bridged structure $P(H)_2Si^+$, which was 16.2 kcal mol^{-1} higher than the open, pyramidal $SiPH_2{}^+$ cation at the MP2(fc)/6-31+G** level of theory, but this energy difference vanished at higher levels of theory.

Parallel to our efforts, Yañez, Ugalde, and co-workers have examined an impressive series of silicon and phosphorus compounds by theoretical means,[21] and most recently a study of the reaction of P^+ with SiH_4 was completed.[22]

In the following, we report the results of a combined theoretical and mass spectrometric study of the relevant parts of the neutral and two low lying cationic [Si, P, H_2] potential-energy surfaces, with particular emphasis on the various isomers, their stabilities and interconversion pathways. Due to the preference for bridged structures with other than first-row elements, special attention is paid to their existence in the [Si, P, H_2] system.

Computational and Experimental Details

The G2 approach has been described in great detail in the literature.[23] Briefly, this composite scheme consists of geometry optimizations at the MP2(full)/6-31G(d) level of theory,[24] followed by a series of single point calculations and empirical corrections to effectively achieve relative energies of zero-point energy corrected with QCISD(T)/6-311+G(3df,2p) quality. Usually, thermochemical data can be reproduced to within ± 2 kcal mol^{-1}, even though cases where such high accuracy cannot be achieved are also known.[25]

In addition to the ab initio MO methods, we performed hybrid DFT/HF calculations employing the modified three-parameter fit of Becke's functional[26] as implemented in the Gaussian 94 code;[27] this will be referred to as B3LYP. Polarized 6-311G(d,p) basis sets were used in these calculations. Recently, it was shown that the B3LYP method is well suited for the description of small organic molecules, and it provides relative energies with an accuracy comparable to G2.[28] However, some controversy can be found in the literature concerning the use of DFT and hybrid DFT/HF methods especially for the calculation of transition structures.[29] Therefore, whenever MP2 and density functional (DFT) optimized structures did not agree with each other, we performed additional CCSD(T)/6-311G(d,p) calculations.

Each stationary point was characterized as a minimum, transition structure (TS), or chemically less relevant higher-order saddle point by the number of negative eigenvalues of the analytically derived MP2/6-31G(d) force constant matrix, from which also the harmonic frequencies, needed for the zero-point-vibration energy (ZPVE) corrections, were obtained. In a few cases, we also computed intrinsic reaction coordinates (IRCs)[30] in order to establish unambiguously the minima connected with a particular TS. All calculations were performed employing Gaussian92[31] and Gaussian94[27] programs.

In several examples, we have previously demonstrated that state-of-the-art tandem mass spectrometry often provides valuable insight into the chemistry of singly and doubly charged cationic, anionic, and neutral silicon compounds.[7b,17,18] Unfortunately, this approach cannot be used for the [Si, P, H_2]$^+$ system under investigation here, because non-resolvable mass overlap prevents the generation of a beam of 'pure' ions in our sector instrument. This failure is due to the small mass difference between silicon and phosphorus, the unfavorable isotope composition of both elements, as well as different amounts of hydrogen incorporation. For example, while chemical ionization of a mixture of PI_3 and silane gives rise to a decent [Si, P, H_2]$^+$ signal, a closer inspection reveals the presence of significant amounts of $Si_2H_n^+$ ions ($n = 1$—5) arising from the ^{28}Si, ^{29}Si, and ^{30}Si isotopes. Electron ionization of possible precursors, e.g. H_3SiPH_2,[32] would not resolve this issue either, because, when using such precursors, the location of the hydrogen atoms in the resulting [Si, P, H_2]$^+$ species is uncertain.

As an alternative, we have performed tandem-mass spectrometry experiments using Fourier-Transform ion cyclotron resonance mass spectrometry (FTICR).[33] Here, ion generation and the subsequent reactions are spatially separated from each other such that the distinction between the isotopologs is not problematic any more. In addition, the mass resolution of this machine is orders of magnitude higher than that of the sector instrument. Thus, after ion generation and transfer to the FTICR cell, prior to any further reactions, $^{28}Si^{+\bullet}$ or $^{31}P^+$ ions were mass-selected, such that isobaric species cannot interfere any more. To this end, the bare atomic cations $^{28}Si^{+\bullet}$ and $^{31}P^+$, respectively, were generated by laser desorption/laser ionization of a pure silicon target and by laser desorption/electron ionization of red phosphorus or electron ionization of gaseous PCl_3. After transferring these ions from the external ion source to the FTICR cell, the isotopes $^{28}Si^{+\bullet}$ and $^{31}P^+$ were mass-selected and thermalized with an excess of pulsed-in deuterium; in the case of silicon cation, collisions with deuterium lead to an efficient removal of the excited state ions $Si^{+\bullet}$ (^4P).[7a,34] Next, the remaining atomic cations were reacted with phosphine and silane, respectively, in order to probe the formation of [Si, P, H_2]$^+$ species. The reactions followed pseudo first-order kinetics; however, because the relative sensitivities of the ion gauge towards these particular gases are unknown, we had to estimate these figures in order to convert these kinetic data into absolute rate constants.[35] Silane and phosphine were generated in an on-line apparatus connected directly to the mass spectrometer by hydrolysis of magnesium silicide and calcium phosphide, respectively, with diluted sulfuric acid and purified by freeze-pump-thaw cycles.

Results and Discussion

As mentioned in the previous section, sector mass spectrometry could not be applied for the characterization of [Si, P, H_2]$^+$ isomers due to mass overlap of isotopologs of [Si_n, P_{2-n}, H_m]$^+$ ($n = 0$—2, $m = 1$—5), and we used Fourier-Transform ion/cyclotron resonance (FTICR) mass spectrometry as an alternative. Despite the fact that FTICR mass spectrometry is a powerful tool in the examination of ion/molecule reactions at ambient temperatures, its capability to differentiate isomeric ions is somewhat limited as compared to that of sector mass spectrometry.[17—19,33,34] Thus, low-energy pathways including rearrangements are favored over the structure-indicative, energy-demanding direct bond cleavages; most importantly, the powerful method of neutralization-reionization mass spectrometry (NRMS)[36] cannot be applied in FTICR. Thus, the access to [Si, P, H_2]$^+$ isomers and their characterization are somewhat limited, and the corresponding neutrals can only be assessed indirectly via thermal electron transfer reactions.

Therefore, we will first present the calculated potential-energy surfaces (PESs) of cationic and neutral [Si, P, H_2]$^{+/0}$ isomers which will serve as a solid basis for the further interpretation of the experimental results obtained with FTICR.

Theoretical

For a comprehensive treatment of the [Si, P, H_2]$^{+/0}$ system and with respect to the experiments conducted, we studied the neutral as well as the singlet and triplet monocationic PESs. The neutral species is likely to exhibit doublet multiplicity, while for the monocation at least two spin states are conceivable, i.e. singlet and triplet electromers. For the sake of simplicity, these structures are indicated according to their respective spin multiplicities and charges; for example, we denote species with the connectivity of a 1-phospha-2-silavinylidene, i.e. P=Si(H)$_2$, **1**, as either the singlet cation $^1\mathbf{1}^+$, the neutral radical $^2\mathbf{1}^\bullet$, or the triplet species $^3\mathbf{1}^+$, respectively.

Neutral [Si, P, H_2]$^\bullet$ Radicals. The neutral 1-phospha-2-silavinylidene radical $^2\mathbf{1}^\bullet$ represents the global minimum on the potential-energy surface of [Si, P, H_2]$^\bullet$ (Scheme 1). The ground state of $^2\mathbf{1}^\bullet$ exhibits $^2B_2$ symmetry and is characterized by a lone-pair as well as a radical center located on the phosphorus atom, together with a formal Si–P dou-

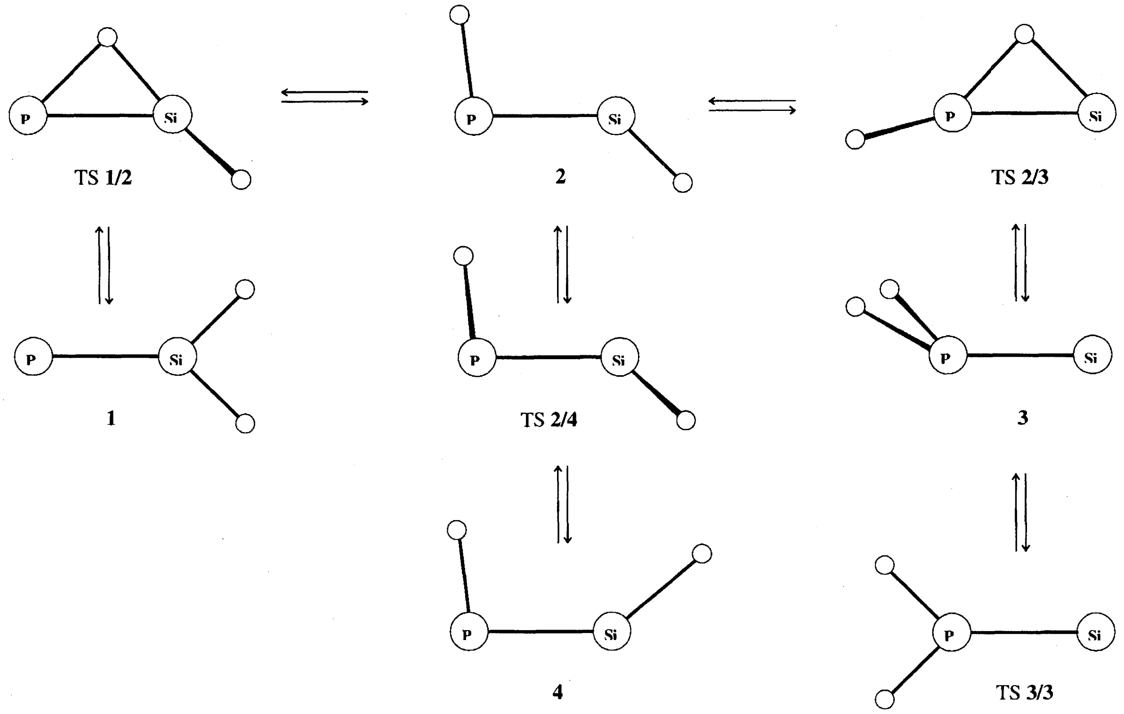

Scheme 1.

ble bond. The singly occupied molecular orbital (SOMO) is an in-plane π-orbital (b_2 in C_{2v}) on the phosphorus. The electron configuration may be written as $b_1^2(\pi)b_2(n)$. The G2 and B3LYP methods predict the Si–P bond length as 2.141 and 2.119 Å, respectively. Similar agreement of both methods holds true for almost all other geometric parameters of the neutral and ionic $[\mathrm{Si, P, H_2}]^{+/0}$ systems (Table 1). However, some notable exceptions will be further discussed below. The planar C_{2v}-symmetrical geometry of $^2\mathbf{1}^\bullet$ is not distorted for the excited states ($^2A_2$: $b_1^2(\pi)a_2(\pi^*)$ and $^2B_1$: $b_2^2(\pi)b_1(n)$). However, at the G2 level these electromers are 28.8 kcal mol^{-1} and 100.1 kcal mol^{-1} higher in energy than the $^2\mathbf{1}^\bullet$ ($^2B_2$) ground state (26.9 and 95.8 kcal mol^{-1} at B3LYP). Though these numbers are not directly related to the further discussion, on a more general note the similarity of the G2 and B3LYP data indicates that the hybrid DFT method might be used with some confidence also for excited states.

A 1,2-H-shift via the transition structure TS $^2\mathbf{1}^\bullet/^2\mathbf{2}^\bullet$ connects $^2\mathbf{1}^\bullet$ with the second low-lying isomer $^2\mathbf{2}^\bullet$. Even though the energy difference between $^2\mathbf{1}^\bullet$ and $^2\mathbf{2}^\bullet$ amounts only to 6.3 kcal mol^{-1} at G2 (4.6 kcal mol^{-1} at B3LYP), both isomers are separated by a reasonable barrier of 30.8 kcal mol^{-1} (29.7 kcal mol^{-1} at B3LYP) relative to $^2\mathbf{1}^\bullet$. TS $^2\mathbf{1}^\bullet/^2\mathbf{2}^\bullet$ exhibits typical features of a transition structure for the hydrogen migration with a P–Si–H angle of 66.2 ° (64.9 ° at B3LYP) and an imaginary frequency ω_i of i1290 cm^{-1} (i1101 cm^{-1} at B3LYP). The fact that the Si–P bond in the *trans* isomer $^2\mathbf{2}^\bullet$ is shorter than in $^2\mathbf{1}^\bullet$ is reflected in the corresponding bond length of TS $^2\mathbf{1}^\bullet/^2\mathbf{2}^\bullet$, which, in contrast to the related $\mathrm{NSiH_2}^\bullet \longrightarrow \mathrm{HNSiH}^\bullet$ rearrangement,[18a,18b)] decreases in the $[\mathrm{Si, P, H_2}]^\bullet$ system.

The *trans* isomer $^2\mathbf{2}^\bullet$ ($^2A'$) where the SOMO is localized on silicon, also deviates in its structure from the nitrogen containing homolog.[18a,18b)] The Si–H bond length (1.484 Å) and the corresponding P–Si–H angle (119.9 °) agree well with the $\mathrm{HSiNH}^\bullet$ analog (1.486 Å and 117.7 °, respectively), while the Si–P–H angle is calculated to be only 94.0 °, as compared to 119.9 ° in $\mathrm{HSiNH}^\bullet$. The rectangular arrangement of the bonding partners indicates a much lower degree of sp^2-hybridization on phosphorus in $^2\mathbf{2}^\bullet$ ($^2A'$) as compared to the case for $\mathrm{HSiNH}^\bullet$. The P–H bond in $^2\mathbf{2}^\bullet$ (1.410 Å) is only slightly shorter as compared to the other isomers (see below), which is pronounced by the relatively high vibrational frequency of the P–H mode (2513 cm^{-1}). Again, the B3LYP calculated parameters are quite similar, i.e. $R_{\mathrm{Si-H}}$: 1.504 Å, $R_{\mathrm{Si-P}}$: 2.088 Å, $R_{\mathrm{P-H}}$: 1.425 Å, α_{PSiH}: 115.6 °, α_{SiPH}: 96.5 °, and ω_{PH}: 2326 cm^{-1}. Thus, we assume that both theoretical methods seem to converge at a reasonable level of confidence, and in the following we will discuss any differences only if these are significant.

The structure of $^2\mathbf{2}^\bullet$ is closely related to its corresponding *cis*-isomer $^2\mathbf{4}^\bullet$ which is marginally higher in energy than the former ($\Delta E = 3.8$ kcal mol^{-1} at G2 and 4.7 kcal mol^{-1} at B3LYP) (Table 2). Except for the configuration, the major difference concerns the P–Si–H angle which is widened to 126.3 ° in the *cis*-isomer as a consequence of the steric repulsion. Interesting in this context is the fact that the existence of the analogous *cis*-isomer of $\mathrm{HSiNH}^\bullet$ could not be verified neither computationally nor experimentally; most probably, it does not represent a minimum on the respective potential-energy surface.[18a,18b)] The barrier connecting $^2\mathbf{2}^\bullet$ and $^2\mathbf{4}^\bullet$ via TS $^2\mathbf{2}^\bullet/^2\mathbf{4}^\bullet$ ($\omega_i = i389$ cm^{-1} at G2 and i494 cm^{-1} at B3LYP) is calculated to be relatively small, i.e. 10.0 kcal mol^{-1} at

Table 1. Geometrical Parameters of the Different Isomers (Bond Lengths R in Ångstrøm and Angles α and Dihedral Angles ω in Degrees).
The first entries correspond to the MP2/6-31G** results used in the G2 procedure, while the second rows show the B3LYP/6-311G** results.

System	R_{SiP}	R_{SiH}	R_{PH}	α_{SiPH}	α_{PSiH}	ω_{HSiPH}
${}^{1}\mathbf{1}^{+}({}^{1}A_1)$	2.112	1.463			118.1	180.0
	2.116	1.478			118.5	180.0
${}^{2}\mathbf{1}^{\bullet}({}^{2}B_2)$	2.141	1.469			122.4	180.0
	2.119	1.483			123.9	180.0
${}^{3}\mathbf{1}^{+}({}^{3}A')$	2.206	1.472			121.6	180.0
	2.218	1.477			121.4	180.0
${}^{2}\mathbf{2}^{\bullet}({}^{2}A')$	2.041	1.484	1.410	94.0	119.9	180.0
	2.088	1.504	1.425	96.5	115.6	180.0
${}^{3}\mathbf{2}^{+}({}^{3}A'')$	2.209	1.476	1.408	95.3	114.9	180.0
	2.248	1.498	1.425	95.7	113.4	180.0
${}^{1}\mathbf{3}^{+}({}^{1}A')$	2.167		1.405	110.5		118.0
	—		—	—		—
${}^{2}\mathbf{3}^{\bullet}({}^{2}A'')$	2.175		1.397	116.1		120.4
	2.205		1.415	113.9		114.5
${}^{3}\mathbf{3}^{+}({}^{3}A_2)$	2.373		1.393	126.9		180.0
	2.399		1.413	127.6		180.0
${}^{2}\mathbf{4}^{\bullet}({}^{2}A')$	2.056	1.485	1.416	88.4	126.3	0.0
	2.096	1.504	1.434	87.4	124.5	0.0
${}^{3}\mathbf{4}^{+}({}^{3}A'')$	2.212	1.487	1.422	90.9	123.8	0.0
	2.256	1.498	1.433	87.8	121.7	0.0
${}^{1}\mathbf{5}^{+}({}^{1}A')$	2.141	1.925	1.464	61.2		96.9
	2.173	2.100	1.471	67.2		94.6
${}^{1}\mathbf{6}^{+}({}^{1}A')$	2.011	1.467	1.500	59.7	167.2	0.0
	2.007	1.403	1.512	62.1	168.9	0.0
${}^{2}\mathbf{7}^{+}({}^{2}A')$	1.970		1.524	59.9		
	2.058		1.489	63.7		
${}^{4}\mathbf{8}^{+}({}^{4}A'')$	2.277	1.493			114.4	
	2.297	1.503			114.5	
${}^{4}\mathbf{9}^{+}({}^{4}A'')$	2.409		1.417	108.7		
	2.421		1.428	107.2		
${}^{2}\mathbf{10}^{+}({}^{2}\Sigma^{+})$	1.908	1.499			180.	
	1.918	1.488			180.	
TS ${}^{2}\mathbf{1}^{\bullet}/{}^{2}\mathbf{2}^{\bullet}$	2.074	1.498	2.036	43.2	122.6	106.7
	2.102	1.506	2.021	44.1	116.0	105.3
TS ${}^{3}\mathbf{1}^{+}/{}^{3}\mathbf{2}^{+}$	2.141	1.470	2.099	42.9	126.1	115.6
	2.184	1.492	2.070	43.1	122.7	109.6
TS ${}^{1}\mathbf{1}^{+}/{}^{1}\mathbf{6}^{+}$	2.051	1.469	2.051	38.3	149.2	180.0
	2.059	1.474	2.059	37.5	148.8	180.0
TS ${}^{2}\mathbf{2}^{\bullet}/{}^{2}\mathbf{3}^{\bullet}$	2.138	1.600	1.425	107.9	52.8	125.4
	2.138	1.639	1.443	102.3	53.8	124.2
TS ${}^{3}\mathbf{2}^{+}/{}^{3}\mathbf{3}^{+}$	2.213	1.619	1.416	107.9	46.3	118.8
	2.260	1.645	1.436	105.4	46.0	114.6
TS ${}^{2}\mathbf{2}^{\bullet}/{}^{2}\mathbf{4}^{\bullet}$	2.192	1.512	1.450	67.8	94.4	73.9
	2.230	1.529	1.447	78.6	98.2	91.7
TS ${}^{3}\mathbf{2}^{+}/{}^{3}\mathbf{4}^{+}$	2.264	1.493	1.428	88.5	116.3	86.4
	2.295	1.506	1.440	83.9	91.4	114.4
TS ${}^{1}\mathbf{3}^{+}/{}^{1}\mathbf{3}^{+}({}^{1}A_1)$	2.143		1.390	123.5		180.0
	2.158		1.406	123.9		180.0
TS ${}^{2}\mathbf{3}^{\bullet}/{}^{2}\mathbf{3}^{\bullet}({}^{2}B_2)$	2.122		1.402	127.3		180.0
	2.140		1.409	127.9		180.0
TS ${}^{1}\mathbf{5}^{+}/{}^{1}\mathbf{5}^{+}({}^{1}A_1)$	2.319	1.676	1.449	45.9		180.0
	2.359	1.691	1.479	45.4		180.0
TS ${}^{1}\mathbf{5}^{+}/{}^{1}\mathbf{6}^{+}$	2.134	1.531	1.493	79.6	83.1	88.1
	2.159	1.530	1.449	77.5	84.4	88.9

G2 and 11.6 kcal mol^{-1} at B3LYP relative to ${}^{2}\mathbf{2}^{\bullet}$. Thus, an experimental probe to distinguish ${}^{2}\mathbf{2}^{\bullet}$ and ${}^{2}\mathbf{4}^{\bullet}$ will not be straightforward and has to account for the facile interconversion of both isomers.

The last minimum found on the neutral potential-energy surface represents the $^{\bullet}SiPH_2$ (${}^{2}A''$) radical ${}^{2}\mathbf{3}^{\bullet}$. The SOMO is located at silicon and represents a π-orbital perpendicular to the symmetry plane. The relative stability of this isomer is comparable with the others and amounts to 9.7 kcal mol^{-1} at G2 and 6.7 kcal mol^{-1} at B3LYP with respect to ${}^{2}\mathbf{1}^{\bullet}$. However, this result is in marked contrast to the nitrogen analog for which the $^{\bullet}SiNH_2$ (${}^{2}A_1$) radical represents the global minimum on the respective potential energy surface.[18a,18b] In addition, the phosphorus compound ${}^{2}\mathbf{3}^{\bullet}$ deviates from planarity with a lowest frequency of 188 cm^{-1} (220 cm^{-1} at B3LYP) corresponding to the bending motion. The low-lying TS ${}^{2}\mathbf{3}^{\bullet}/{}^{2}\mathbf{3}^{\bullet}$ (${}^{2}B_2$) for degenerate conversion exhibits a planar structure and is only 0.6 kcal mol^{-1} higher in energy than ${}^{2}\mathbf{3}^{\bullet}$, with an imaginary frequency of *i*340 cm^{-1} (*i*269 cm^{-1} at B3LYP). However, the isomer ${}^{2}\mathbf{3}^{\bullet}$ resides in a relatively deep well and is separated from ${}^{2}\mathbf{2}^{\bullet}$ by a reasonably high barrier TS ${}^{2}\mathbf{2}^{\bullet}/{}^{2}\mathbf{3}^{\bullet}$, which demands 21.7 kcal mol^{-1} at G2 and 22.8 kcal mol^{-1} at B3LYP relative to ${}^{2}\mathbf{2}^{\bullet}$. Interestingly, the trend in stabilities of the isomers in the neutral [Si, P, H_2]$^{\bullet}$ system differs quite significantly from that in the nitrogen case.[18a,18b]

Triplet [Si, P, H_2]$^+$ Cations. The triplet potential-energy surface of the cation [Si, P, H_2]$^+$ exhibits many similarities with the neutral system. Conceptually, this result is not really surprising because ionization to the triplet state involves the removal of an electron from a high-lying, weakly bonding π orbital or from a lone-pair on either Si or P. Consequently, many structural features are to a first approximation not affected as will be shown. Hence, the connectivities and intramolecular interconversions of the triplet cations of [Si, P, H_2]$^+$ can also be represented by Scheme 1.

As for the neutral system, the most stable isomer on the triplet surface corresponds to 1-phospha-2-silavinylidene cation ${}^{3}\mathbf{1}^{+}$ (${}^{3}A_2$), whose configuration is generated by an electron removal from an π_{SiP} bonding orbital (b_1). The structure of ${}^{3}\mathbf{1}^{+}$ is only slightly affected by the ionization as compared to neutral ${}^{2}\mathbf{1}^{\bullet}$. The Si–P bond somewhat elongates upon ionization (2.206 Å), while the SiH_2 substructure is hardly perturbed (Table 1). This is in line with the appearance of only small changes in the corresponding vibrational frequencies for the symmetrical and asymmetrical Si–H stretching (a_1: 2395 cm^{-1} and b_2: 2444 cm^{-1}), which are just marginally different from those of neutral ${}^{2}\mathbf{1}^{\bullet}$ (a_1: 2348 cm^{-1} and b_2: 2382 cm^{-1}). The corresponding adiabatic ionization energy (${}^{2}\mathbf{1}^{\bullet} \longrightarrow {}^{3}\mathbf{1}^{+}$) is calculated to 8.93 eV using G2 (8.82 eV with B3LYP).

The transition structure TS ${}^{3}\mathbf{1}^{+}/{}^{3}\mathbf{2}^{+}$ connecting ${}^{3}\mathbf{1}^{+}$ with the *trans* isomer ${}^{3}\mathbf{2}^{+}$ is also quite similar to the corresponding neutral TS, both representing typical hydrogen-bridged systems. With respect to ${}^{3}\mathbf{1}^{+}$, TS ${}^{3}\mathbf{1}^{+}/{}^{3}\mathbf{2}^{+}$ is less stable by 31.8 kcal mol^{-1} (31.5 kcal mol^{-1} at B3LYP), i.e. reasonably high enough in energy to prevent a facile interconversion of

Table 2. Total (E_{tot}) and Relative (ΔE) Energies of the Individual Isomers and the Associated Transition Structures

The total energies for G2 values and B3LYP/6-311G** results are given in Hartree while the ZPVE and relative stabilities ΔE are given in kcal mol^{-1}.

System	E_{tot} (G2)	ZPVE	ΔE (G2)	E_{tot} (B3LYP)	ZPVE	ΔE (B3LYP)
$^{1}\mathbf{1}^{+}(^{1}A_{1})$	−630.759900	10.20	31.7	−631.692523	9.58	29.4
$^{2}\mathbf{1}^{\bullet}(^{2}B_{2})$	−631.094327	10.18	−178.2	−632.029953	9.49	−182.4
$^{3}\mathbf{1}^{+}(^{3}A')$	−630.766163	10.59	27.7	−631.706062	10.00	20.9
$^{2}\mathbf{2}^{\bullet}(^{2}A')$	−631.084223	10.52	−171.8	−632.022588	9.66	−177.8
$^{3}\mathbf{2}^{+}(^{3}A'')$	−630.755350	10.24	34.5	−631.697951	9.37	26.0
$^{1}\mathbf{3}^{+}(^{1}A')$	−630.801924	10.53	5.3	—	—	—
$^{2}\mathbf{3}^{\bullet}(^{2}A'')$	−631.078783	10.84	−168.4	−632.019339	10.22	−175.7
$^{3}\mathbf{3}^{+}(^{3}A_{2})$	−630.749263	10.58	38.4	−631.693927	9.65	28.5
$^{2}\mathbf{4}^{\bullet}(^{2}A')$	−631.078033	10.26	−168.0	−632.015134	9.51	−173.1
$^{3}\mathbf{4}^{+}(^{3}A'')$	−630.752146	9.87	36.5	−631.690888	9.24	30.4
$^{1}\mathbf{5}^{+}(^{1}A')$	−630.810382	10.72	0.0	−631.739313	9.69	0.0
$^{1}\mathbf{6}^{+}(^{1}A')$	−630.789365	9.77	13.2	−631.717307	9.23	13.8
$^{2}\mathbf{7}^{+}(^{2}A')$	−630.167726	1.89	—	−631.094645	4.75	—
$^{4}\mathbf{8}^{+}(^{4}A'')$	−630.127199	4.18	—	−631.059400	4.40	—
$^{4}\mathbf{9}^{+}(^{4}A'')$	−630.116533	4.15	—	−631.050703	4.42	—
$^{2}\mathbf{10}^{+}(^{2}\Sigma^{+})$	−630.081317	4.98	—	−631.005335	5.10	—
TS $^{2}\mathbf{1}^{\bullet}/^{2}\mathbf{2}^{\bullet}$	−631.045259	8.74	−147.4	−631.982606	8.21	−152.7
TS $^{3}\mathbf{1}^{+}/^{3}\mathbf{2}^{+}$	−630.715438	8.73	59.6	−631.655885	8.11	52.4
TS $^{1}\mathbf{1}^{+}/^{1}\mathbf{6}^{+}$	−630.759797	9.21	31.7	−631.689133	8.87	31.5
TS $^{2}\mathbf{2}^{\bullet}/^{2}\mathbf{3}^{\bullet}$	−631.049581	8.71	−150.1	−631.986315	7.99	−155.0
TS $^{3}\mathbf{2}^{+}/^{3}\mathbf{3}^{+}$	−630.714466	8.54	60.2	631.652973	7.77	54.2
TS $^{2}\mathbf{2}^{\bullet}/^{2}\mathbf{4}^{\bullet}$	−631.068269	8.56	−161.8	−632.004224	7.87	−166.2
TS $^{3}\mathbf{2}^{+}/^{3}\mathbf{4}^{+}$	−630.742998	8.89	42.3	−631.684284	8.14	34.5
TS $^{1}\mathbf{3}^{+}/^{1}\mathbf{3}^{+}$	−630.799939	10.31	6.6	−631.734831	9.75	2.8
TS $^{2}\mathbf{3}^{\bullet}/^{2}\mathbf{3}^{\bullet}$	−631.078310	10.92	−168.1	−632.018444	9.89	−175.2
TS $^{1}\mathbf{5}^{+}/^{1}\mathbf{5}^{+}$	−630.771446	11.59	24.4	−631.697563	10.43	26.2
TS $^{1}\mathbf{5}^{+}/^{1}\mathbf{6}^{+}$	−630.766522	9.08	27.5	−631.697824	8.31	26.0

both ions. While G2 and B3LYP calculations lead to similar results with regard to structural features, for both the neutrals and triplet cations, the two methods disagree in the computation of the imaginary frequencies for TS $^{2}\mathbf{1}^{\bullet}/^{2}\mathbf{2}^{\bullet}$ and TS $^{3}\mathbf{1}^{+}/^{3}\mathbf{2}^{+}$. Thus, G2 predicts $i1812$ cm^{-1} for the cationic TS as compared to only $i1289$ cm^{-1} in the neutral, while the B3LYP calculated frequencies agree nicely for both cases, being $i1101$ cm^{-1} and $i1155$ cm^{-1} for the neutral and the triplet state of the cation, respectively. We suspect that this difference is due to the limited geometry optimization in the G2 scheme which is restricted to second order Møller-Plesset perturbation theory.

The *trans* isomer $^{3}\mathbf{2}^{+}$ ($^{3}A''$) shows also many similarities to neutral $^{2}\mathbf{2}^{\bullet}$ with almost rectangular Si–P and P–H bonds as the dominant feature. However, the Si–P bond is significantly elongated as compared to that in the neutral radical $^{2}\mathbf{2}^{\bullet}$ ($\Delta R_{\mathrm{Si-P}} = 0.168$ Å at G2 and 0.160 Å at B3LYP). The bond elongation results from the ionization from the π orbital (a$''$). Similar to the neutral surface, the *trans*-isomer $^{3}\mathbf{2}^{+}$ is only 6.7 kcal mol^{-1} (5.1 kcal mol^{-1} at B3LYP) less stable than $^{3}\mathbf{1}^{+}$, which is the lowest-lying isomer on the triplet potential energy surface. Another electromer with the same connectivity corresponds to $^{3}\mathbf{2}^{+}$ ($^{3}A'$), which is 32.4 kcal mol^{-1} higher in energy (at G2) as compared to $^{3}\mathbf{2}^{+}$ ($^{3}A''$). This excited state $^{3}\mathbf{2}^{+}$ ($^{3}A'$) is characterized by a shorter Si–P bond ($R_{\mathrm{Si-P}} = 2.076$ Å) and an enlarged Si–P–H angle (126.8 °), both indicative of an sp^{2} hybridization at phosphorus. Similarly, for the *cis* isomer $^{3}\mathbf{4}^{+}$, two electronic states ($^{3}A''$ and $^{3}A'$) were found, whose structural features are quite similar. The $^{3}A''$ state is the more stable one and is just 8.8 kcal mol^{-1} (9.5 kcal mol^{-1} at B3LYP) less stable than $^{3}\mathbf{1}^{+}$, while the G2 calculations predict $^{3}\mathbf{4}^{+}$ ($^{3}A'$) to be 29.7 kcal mol^{-1} more energetic than $^{3}\mathbf{1}^{+}$. *Cis–trans* isomerization can proceed via TS $^{3}\mathbf{2}^{+}/^{3}\mathbf{4}^{+}$, in which the Si–P bond length is somewhat elongated, while the corresponding imaginary frequency is again close to that of the neutral ($i396$ cm^{-1} at G2 and $i442$ cm^{-1} at B3LYP). The associated barrier is even lower than in the neutral system and amounts to only 7.8 kcal mol^{-1} (8.6 kcal mol^{-1} at B3LYP) relative to $^{3}\mathbf{2}^{+}$.

The last isomer of importance on the triplet surface corresponds to 2-phopha-1-silavinylidene cation $SiPH_2^{+}$ ($^{3}\mathbf{3}^{+}$). The isomer $^{3}\mathbf{3}^{+}$ ($^{3}A_{2}$) is characterized by a planar, C_{2v} symmetrical structure with an elongated Si–P bond (2.373 Å at G2 and 2.399 Å at B3LYP) while the related neutral $^{2}\mathbf{3}^{\bullet}$ is C_{s}-symmetric ($R_{\mathrm{Si-P}} = 2.175$ Å at G2 and 2.205 Å at B3LYP, respectively). Accordingly, the lowest frequency of $^{3}\mathbf{3}^{+}$ is found to correspond to the out-of-plane distortion (249 cm^{-1} at G2). Though $^{3}\mathbf{3}^{+}$ is computed to be slightly less stable (G2:

3.8 kcal mol^{-1} and B3LYP: 2.5 kcal mol^{-1}) than ^{3}**2**$^+$, the corresponding interconversion process via TS ^{3}**2**$^+$/^{3}**3**$^+$ is associated with a sizeable activation barrier (G2 : 25.6 kcal mol^{-1} and B3LYP: 28.2 kcal mol^{-1} with respect to ^{3}**2**$^+$) such that a distinction of the two isomers should be possible, provided an independent generation of both species is achieved.

Singlet [Si, P, H_2]$^+$ Cations. As already stressed in the beginning of this paper, our particular interest in the [Si, P, H_2]$^{+/0}$ systems is the search for non-classical structures. Due to the fact that the [Si, P, H_2]$^+$ cations are isoelectronic with the [Si_2, H_2] system, where the existence of hydrogen-bridged minima is well established already,[9—15] we suggested that similar structures should exist also for the phosphorus containing species. Analogs to the doubly-bridged disilyne structure were indeed found computationally on the singlet surface of [Si, P, H_2]$^+$.[19,20,22]

The results of our calculations for the singlet manifold of [Si, P, H_2]$^+$ are summarized in Scheme 2, and the related geometrical data are given in Table 1. In general, the singlet potential-energy surface differs entirely from the neutral radical and the cationic triplet surfaces. Thus, the HSiPH structures ^{1}**2**$^+$ and ^{1}**4**$^+$ do not represent minima on the cationic singlet PES. Instead, the most stable isomer ^{1}**5**$^+$ ($^1A'$) exhibits an asymmetrical doubly-bridged structure, which represents a transition structure on the two other surfaces. Thus, ^{1}**5**$^+$ exhibits a non-classical cyclic structure, in which, however, the hydrogen atoms are more strongly bound to phosphorus while the Si–H bonds are rather long, i.e. 1.925 Å at G2 and 2.100 Å at B3LYP; note that the significant deviation between the two results again highlights the limitations of the G2 procedure due to its dependence on MP2 geometries. The most stable singlet structure ^{1}**5**$^+$ lies below the most stable triplet structure ^{3}**1**$^+$ by 27.7 kcal mol^{-1} (B3LYP: 20.9 kcal mol^{-1}).

In a recent paper, Schoeller and Busch[20] pointed out that the relative stability of ^{1}**5**$^+$ is strongly dependent on the computational level. As this aspect is crucial for the evaluation of non-classical structures, we investigated this particular issue in more detail. The major point, raised by Schoeller and Busch, concerns the relationship of the doubly-bridged isomer ^{1}**5**$^+$ and the corresponding acyclic, classical structure ^{1}**3**$^+$, for which the energy differences rapidly decrease when going from the HF level to correlated methods; this difference vanishes at the QCISD(T) level. While this huge effect is not confirmed at the levels used presently, the trend remains the same. When using the standard G2 procedure (i.e. relying on the MP2 optimized structures), ^{1}**5**$^+$ ($^1A'$) turns out to be by 5.3 kcal mol^{-1} more stable than ^{1}**3**$^+$ ($^1A'$). However, the first problem we are facing is that the acyclic isomer ^{1}**3**$^+$ does not represent a minimum on the B3LYP/6-311G** surface. Using the angle Ω between the Si–P bond and the $P(H)_2$ plane as a coordinate and optimizing all the remaining geometrical parameters at each step for Ω between 0 ° and 180 °, we have obtained the energy profiles as shown in Fig. 1.

The MP2(full)/6-31G** curve clearly reveals a preference for ^{1}**5**$^+$ ($^1A'$) as the most stable isomer, while around $\Omega = 110°$ a second minimum appears, which, however, is just 1.5 kcal mol^{-1} lower than the highest point in the energy scan which can formally be assigned to TS ^{1}**3**$^+$/^{1}**3**$^+$. In distinct contrast, the B3LYP/6-311G** calculations lead to a single minimum along the coordinate Ω and show only a

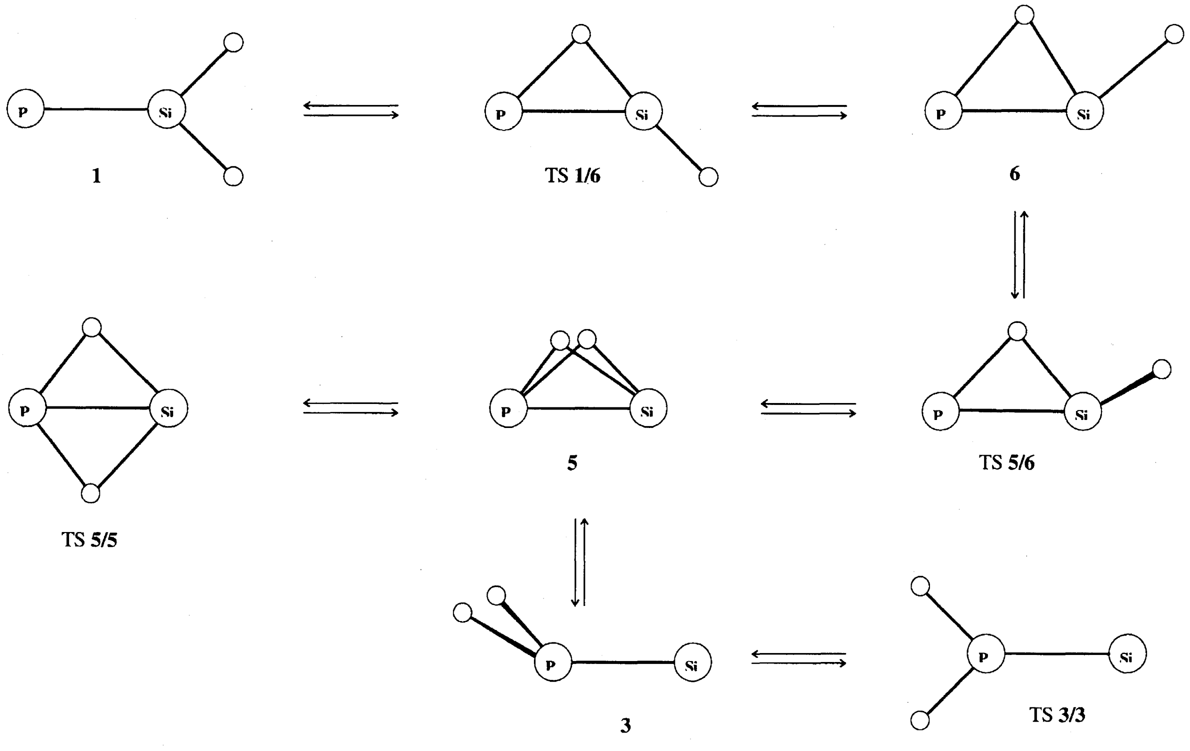

Scheme 2.

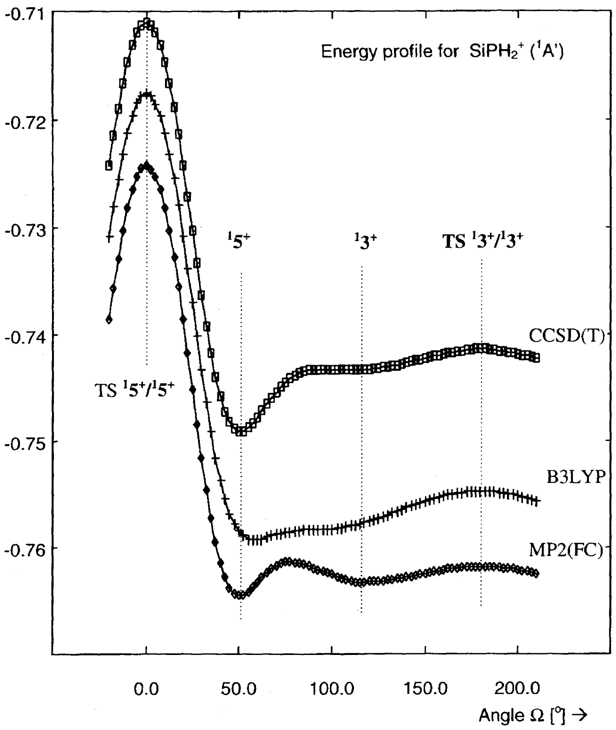

Fig. 1. The calculated potential energy scan for the symmetric Si–P–H bending coordinate Ω. The energy is in hartree and the individual curves are shifted arbitrarily in energy.

shoulder in the energy profile for $\Omega\approx108°$, i.e. the region where the minimum $^1\mathbf{3}^+$ is predicted by the MP2 geometry-based G2 method. In order to tackle this problem further, we employed the more reliable CCSD(T) method together with 6-311G** basis sets for the same type of calculations. The well of the doubly-bridged structure $^1\mathbf{5}^+$ appears now more pronounced, while instead of the second minimum corresponding to $^1\mathbf{3}^+$ is only a plateau, which connects $^1\mathbf{5}^+$quite smoothly. Even though the basis sets we used are by far too small to give a definitive answer, we suspect that $^1\mathbf{3}^+$ does not represent a stable species if the zero-point-energy is taken into account and if larger basis sets would be applied in the optimization procedure. Therefore, we have not further attempted to localize the corresponding TS $^1\mathbf{3}^+/^1\mathbf{5}^+$ for the mutual interconversion of the two isomers at the G2 level of theory.

The pronounced energy increase at $\Omega=0$, seen at all levels of theory Fig. 1, corresponds to the butterfly vibration which inverts $^1\mathbf{5}^+$ via TS $^1\mathbf{5}^+/^1\mathbf{5}^+$. This planar transition structure is 24.4 kcal mol^{-1} (26.2 kcal mol^{-1} at B3LYP) less stable than $^1\mathbf{5}^+$. The Si–P bond length is significantly elongated to 2.319 Å (2.359 Å at B3LYP), while the P–H bond remains almost unchanged. The associated imaginary frequency of *i*984 cm^{-1} (*i*943 cm^{-1} at B3LYP) for this TS is very close to the corresponding frequency in disilyne (*i*905 cm^{-1}).[15b)]

As far as the connection of the doubly-bridged structure with the rest of the singlet PES is concerned, a mono-bridged structure could be located. The minimum $^1\mathbf{6}^+$ ($^1A'$) is planar with both hydrogen atoms cis to the Si–P bond and one P–Si–H angle of 167.2 ° (168.6 ° at B3LYP) and the other 45.9 ° (46.3 ° at B3LYP). Structure $^1\mathbf{6}^+$ shows some similarities to the mono-bridged Si(H)SiH isomer recently reported by Grev and Schaefer (cf. Structure VIII in Ref. 15b). As compared to the corresponding doubly-bridged structure $^1\mathbf{5}^+$, the Si–P bond in $^1\mathbf{6}^+$ is somewhat shorter, while the P–H bond to the bridging hydrogen is elongated accordingly. Similar differences between mono- and doubly bridged structures were found for the silicon analogs, and thus, it is not surprising that also the relative stability of $^1\mathbf{6}^+$ (10.6 kcal mol^{-1} at G2 and 7.6 kcal mol^{-1} at B3LYP, respectively) matches the corresponding energy difference found in disilyne (8.7 kcal mol^{-1}); note that, irrespective of the level of theory used in the previous and present studies, the non-classical structures represent minima. It seems that in $^1\mathbf{6}^+$ the mono-bridged bonding situation is even more pronounced, because the lowest (out-of-plane) frequency (285 cm^{-1} at MP2 and 294 cm^{-1} at B3LYP) is larger as that found for the non-classical disilyne isomers (108 cm^{-1}).[15b)]

The isomerization from $^1\mathbf{5}^+$ to $^1\mathbf{6}^+$ can proceed via the non-planar transition structure TS $^1\mathbf{5}^+/^1\mathbf{6}^+$, which is found to be 27.5 kcal mol^{-1} (26.0 kcal mol^{-1} at B3LYP) higher in energy than the global minimum $^1\mathbf{5}^+$. This value is significantly higher than that proposed for the silicon analog (12.4 kcal mol^{-1}), and can be traced back to the larger polarity of the Si–P bond. The calculated harmonic frequencies of TS $^1\mathbf{5}^+/^1\mathbf{6}^+$ have imaginary components at all computational levels applied in this study (SCF: *i*371 cm^{-1}, MP2: *i*886 cm^{-1}, and B3LYP: *i*609 cm^{-1}). Thus, the two different isomers might be experimentally distinguishable.

We have not succeeded in locating a singlet structure for a non-bridged HSiPH, similar to structures **2** and **4**, neither on the MP2 nor on the B3LYP surfaces. The only other isomer connected to $^1\mathbf{6}^+$ corresponds to the C_{2v} symmetrical structure $^1\mathbf{1}^+$ ($^1A_1$). It is connected to $\mathbf{6}^+$ by the planar transition structure TS $^1\mathbf{1}^+/^1\mathbf{6}^+$ which is 31.7 kcal mol^{-1} (31.5 kcal mol^{-1} at B3LYP) higher than the global minimum $^1\mathbf{5}^+$, having an imaginary frequency of *i*474 cm^{-1} (*i*395 cm^{-1} with B3LYP). Note, that the singlet isomer $^1\mathbf{1}^+$ is even 3.9 kcal mol^{-1} (5.2 kcal mol^{-1} with B3LYP) *higher* in energy than the corresponding triplet cation $^3\mathbf{1}^+$; the latter is also the most stable species on the triplet potential energy surface.

Finally, we briefly examined the minima on the doublet

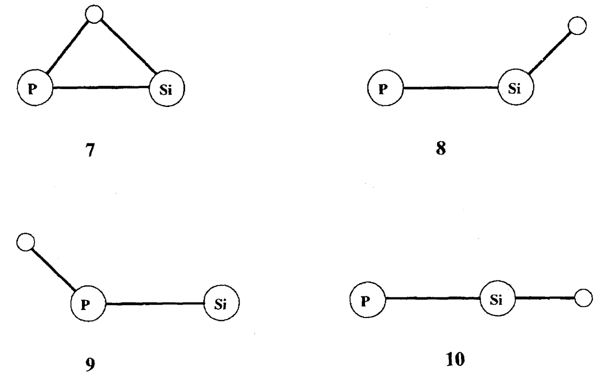

Scheme 3.

surface of the [Si, P, H]$^+$ cation, because this particular ion arises as a product in the ion/molecule reactions (see below). G2 theory as well as B3LYP predict the global minimum of the [Si, P, H]$^+$ potential-energy surface as the non-classical, bridged structure $^2\mathbf{7}^{+\bullet}$ ($^2A'$) (Scheme 3). At the G2 level of theory, the heat of formation of $^2\mathbf{7}^{+\bullet}$ ($^2A'$) is predicted to be 275 kcal mol^{-1}.[37)] The classical, acyclic structures HSiP$^{+\bullet}$, $^4\mathbf{8}^{+\bullet}$ ($^4A''$), and HPSi$^{+\bullet}$, $^4\mathbf{9}^{+\bullet}$ ($^4A''$), belong to the quartet surface and are significantly higher in energy, i.e. 25.4 and 32.1 kcal mol^{-1}, respectively (22.1 and 27.6 kcal mol^{-1} with B3LYP). The only acyclic structure which could be located on the doublet potential-energy surface corresponds to linear HSiP$^{+\bullet}$, $^2\mathbf{10}^{+\bullet}$ ($^2\Sigma^+$). However, this higher homolog of hydrogen cyanide cation radical is 54.2 kcal mol^{-1} higher in energy than the non-classical structure $^2\mathbf{7}^{+\bullet}$ ($^2A'$).

Experimental

As outlined above, our experimental means had to be confined to FTICR studies of the [Si, P, H_2]$^+$ system, because sector mass spectrometry failed due to non-resolvable isobaric multiplets.

From a conceptual point of view, many gas-phase routes to [Si, P, H_2]$^+$ are conceivable. However, we concentrated our efforts on those reactions which can potentially occur in the interstellar environments. Further restrictions in the choice of the reactants arise from the fact that our experimental set-up allows us to examine reactions of (almost any) ions with only the neutrals which are available as macroscopically stable precursors at room temperature. Thus, we decided to study the fundamental reactions (1) and (2) by means of the FTICR technique.

$$Si^{+\bullet} + PH_3 \longrightarrow \text{products} \qquad (1)$$

$$P^+ + SiH_4 \longrightarrow \text{products} \qquad (2)$$

These two reactions comprise four reactants which are likely to exist in heavy-element rich interstellar media, i.e. atomic cations and neutral element hydrides.[4)] The latter hydrides can probably be formed in astrochemical processes,[4)] though phosphine has not yet been detected.[38)] Further, both reactions can lead to the formation of [Si, P, H_2]$^+$ via stabilization of the excited association complexes [$Si^{+\bullet}\cdot PH_3$] and [$P^+\cdot SiH_4$] by expulsion of atomic or molecular hydrogen.

Reaction of Si$^{+\bullet}$ with Phosphine. Under FTICR conditions, reaction (1) occurs quite efficiently. Due to the lack of parameters for determining the sensitivity of the ion gauge toward phosphine, we cannot give a precise figure for the absolute pressure of the neutral reactant in reaction (1). However, we can estimate the relative sensitivity[35)] leading to a rate constant of $k_1=(1.0\pm0.5)\cdot10^{-9}$ cm^3 s^{-1}, which is close to the collisional limit ($k_C=1.4\cdot10^{-9}$ cm^3 s^{-1}). Thus, due to the high cross section of reaction (1) and the fact that ground state Si$^{+\bullet}$ does react with the omnipresent H_2, formation of [Si, P, H_n]$^+$ (n=1,2) may occur in interstellar media whenever enough silicon and phosphorus are present.

Experimentally, three different product channels are observed (reactions 1a—1c).

$$Si^{+\bullet} + PH_3 \longrightarrow [Si, P, H_2]^+ + H^\bullet \qquad (1a)$$

$$Si^{+\bullet} + PH_3 \longrightarrow [Si, P, H]^{+\bullet} + H_2 \qquad (1b)$$

$$Si^{+\bullet} + PH_3 \longrightarrow SiH^+ + PH_2^\bullet \qquad (1c)$$

The branching ratio between reactions (1a) and (1b) amounts to ca. 3 : 7, and the [Si, P, H_2]$^+$ cation intensity is further depleted by a consecutive reaction of this ion with residual water in the vacuum system to yield the very stable SiOH$^+$ cation[18c,18d)] concomitant with neutral phosphine. The cation radical [Si, P, H]$^{+\bullet}$, however, leads subsequently to higher adducts [Si, P_2,H_n]$^{+\bullet}$ (n=0,2) upon further reaction with phosphine, as established by applying double resonance techniques. In addition, formation of SiH$^+$ via reaction (1c) is observed to some extent, whenever the precursor Si$^{+\bullet}$ ions were not completely quenched (see below).

Silicon cation Si$^{+\bullet}$ exhibits a ^{2}P ground state (3s^2 3p^1). Thus, the homolytic cleavage reaction (1a) may lead to either singlet or triplet states of [Si, P, H_2]$^+$. On the other hand, reaction (1b) should lead to a doublet state of [Si, P, H]$^{+\bullet}$. Reaction (1c) can arise from electronically excited Si$^{+\bullet}$ (^{4}P) as well as from kinetically 'hot' ground state Si$^{+\bullet}$ (^{2}P). Interestingly, the occurrence of reaction (1c) can only be suppressed after thorough thermalization of silicon cation by excessive treatment with pulsed-in deuterium (which converts Si$^{+\bullet}$ (^{4}P) into SiD$^+$)[7a,34)] and additional thermalization with argon as a pulsed-in buffer gas as well as the leaked-in phosphine. If these thermalization procedures are applied until completion, the remaining, mass-selected Si$^{+\bullet}$ ions do not undergo reaction (1c) anymore; this is completely in line with the endothermicity of this process (see below). While the occurrence of reaction (1c) for the Si$^{+\bullet}$ (^{4}P) is not very surprising, and because this excited state can easily be removed from the Si$^{+\bullet}$ population by reaction with deuterium, the sensitivity of the ground state Si$^{+\bullet}$(^{2}P) towards SiH$^+$ formation with phosphine should be addressed in some more detail. According to thermochemistry literature,[39)] reaction (1c) is 7.9 kcal mol^{-1} endothermic, and thus, it should not occur for thermalized ions as is indeed confirmed experimentally. However, the experimental thermochemistry for these highly unsaturated species is not always precisely known. In order to clarify this particular issue further, we surveyed recent ab initio studies, and according to G2 calculations, the reaction endothermicity amounts to no more than 5.1 kcal mol^{-1}.[18c,23)] Considering the fact that reaction (1c) can be represented as a direct hydrogen atom abstraction without any further structural rearrangements, it is rather likely that its cross section becomes high whenever it is thermochemically accessible. In contrast, generation of [Si, P, H_2]$^+$ and [Si, P, H]$^{+\bullet}$ require Si–P bond formation, and thus, a longer lifetime is required for the association complex [$Si^{+\bullet}\cdot PH_3$] formed initially. Moreover, reaction (1b) is only exothermic when molecular hydrogen is formed as a neutral product, and thus, it will also involve an entropically disfavored TS for elimination of hydrogen. Further, the thermochemistry outlined above for [Si, P, H]$^{+\bullet}$ implies that for thermalized Si$^{+\bullet}$ (^{2}P) reaction (1b) must involve the formation of the non-classical isomer $^2\mathbf{7}^{+\bullet}$ ($\Delta H_R=-22$ kcal mol^{-1}), such that the reactants' connectivities are nearly completely disintegrated in the course of product formation.

Let us now consider the formation of [Si, P, H_2]$^+$ in some more detail. The pertinence of reaction (1a) upon excessive thermalization of silicon cation reveals that this product ion arises from thermalized Si$^{+\bullet}$ in its ^{2}P ground state. In order to relate this observation to the calculated PES of the [Si, P, H_2]$^+$ system, we first need an absolute reference in order to convert the G2 energies into heats of formation.[18c,37)] For this purpose, we have chosen isomer $^3\mathbf{3}^+$ for which we can adopt a heat of formation ($\Delta H^\circ{}_f$) of 276 kcal mol^{-1} according to the careful G2 study of Ugalde and co-workers.[22)] At thermal conditions, the entrance channel of reaction (1) is located at 297 kcal/mol.[39)] Due to the fact that reaction (1a) demands loss of a hydrogen atom ($\Delta H^\circ{}_f=52$ kcal mol^{-1}), formation of [Si, P, H_2]$^+$ can only occur when the species formed obeys $\Delta H^\circ{}_f$ ([Si, P, $H_2]^+$) $\leq$245 kcal mol^{-1}. With respect to the theoretical results, this finding readily implies that only $^1\mathbf{3}^+$ and/or $^1\mathbf{5}^+$ are accessible, because only for these isomers is the thermodynamic condition fulfilled. Considering the above discussion on the "stability" of the classical structure $^1\mathbf{3}^+$, we can quite certainly conclude that the bridged cation $^1\mathbf{5}^+$ must evolve as the only product of reaction (1a).

This conjecture sheds further light on the efficient competition of the endothermic reaction (1c) with reactions (1a) and (1b). Thus, not only loss of molecular hydrogen to afford $[Si, P, H]^{+\bullet}$, but also the formally simple loss of a hydrogen atom to yield $[Si, P, H_2]^+$ is probably associated with a kinetic barrier, because the formation of the bridged structure $^1\mathbf{5}^+$ requires significant structural changes and substantial atomic displacements with respect to the reactants in reaction (1). Instead, reaction (1c) must not involve any Si–P bond formation and can occur with a huge efficiency, once the threshold energy for simple hydrogen atom transfer from PH_3 to $Si^{+\bullet}$ is provided. Notwithstanding these dynamic restrictions, reaction (1) occurs quite rapidly for thermalized reactants, so the associated kinetic barriers cannot be insurmountably high. The suggestion that reaction (1a) may be associated with a kinetic barrier further accounts for the larger propensity of dehydrogenation (reaction 1b) as compared to the formally simple loss of a hydrogen atom in that both reactions must involve significant reorganization, and reaction (1b) is simply more exothermic ($\Delta H_R=-22$ kcal mol^{-1}) than reaction (1a) which leads to the formation of $[Si, P, H_2]^+$ ($\Delta H_R=-8$ kcal mol^{-1}).

Further, we briefly examined the correspondence of the $[Si, P, H_2]^+$ cation formed in reaction (1a) to its neutral counterpart by means of bracketing the ionization energy (IE) of $[Si, P, H_2]^\bullet$ in thermal electron transfer from neutral substrates with known IEs[39] to the cation forming ion reaction (1a). Thus, we found that the $[Si, P, H_2]^+$ ion formed undergoes electron transfer with aniline (*IE*=7.7 eV) to afford aniline cation radical and neutral $[Si, P, H_2]^\bullet$, while no electron transfer occurred with toluene (*IE*=8.8 eV). With regard to the calculated adiabatic *IE* of 7.7 eV (7.9 eV with B3LYP) for the transition $\mathbf{1}\ (^2B_2) \longrightarrow {}^1\mathbf{5}^+\ (^1A')$, this observation agrees with formation of the bridged singlet $[Si, P, H_2]^+$ cation. However, we have not pursued this issue any further with respect to the other isomers on the singlet potential-energy surface, because the FTICR technique does not allow any information about the neutral species formed. This information would indeed be essential, because our theoretical results demonstrate that the structural differences between the singlet cation and the doublet state of the neutral congener are quite large. Hence, the assumption of adiabatic electron transfer to the most stable neutral is not straightforward, and further interpretation of the results is prohibited unless evidence for the neutral structure is available.

Reaction of $P^{+\bullet}$ with Silane An entirely different product distribution results for reaction (2) which occurs under FTICR conditions practically at the collisional limit, i.e. $k_2=(1.4\pm0.6)\cdot10^{-9}$ cm^3 s^{-1} versus $k_C=1.5\cdot10^{-9}$ cm^3 s^{-1}. No evidence for Si–P bond formation is observed and the exclusive products arise from successive hydrogen transfers (reactions 2a and 2b).

$$P^+ + SiH_4 \rightarrow SiH_3{}^+ + PH \qquad (2a)$$

$$P^+ + SiH_4 \rightarrow PH_2{}^+ + SiH_2 \qquad (2b)$$

The branching ratio between reactions (2a) and (2b) amounts to 9 : 1, perfectly reflecting the associated reaction exothermicities (-33.3 and -17.4 kcal mol^{-1}, respectively)[39] as well as the extent of atom transfer required in both reactions. Note that reaction (2a) will escape experimental observation in many experimental setups because reactant and product ions are isobaric (both 31 amu). However, the mass resolution capability of the FTICR technique in MS^n experiments is more than sufficient to resolve this mass difference, i.e. $m/z(P^+)=30.97376$ amu versus $m/z(SiH_3^+)=31.00040$, thus, $m/\Delta m\approx1200$, as compared to a nominal mass resolution of the instrument, exceeding by far $m/\Delta m>10^6$.

From a chemical point of view, the outcome of reaction (2) is intriguing. Phosphorus cation bears a triplet ground state (^3P). Thus, dehydrogenation of the closed-shell species silane by P^+ must give rise to triplet $^3[Si, P, H_2]^+$ species as long as spin conservation is maintained (and molecular hydrogen is formed as a neutral). Only curve crossing, for example via spin-orbit-coupling or a predissociative mechanism, would give access to the lower lying singlet surface. Experimentally, the hydrogen transfer reactions (2a) and (2b) take place exclusively, and no evidence for Si–P bond formation is observed. This finding fully agrees with the conjecture that curve crossing is negligible in the ion chemistry of silicon and phosphorus,[18c)] at least as far as fast ion/molecule reactions are concerned.

Further, the apparent non-occurrence of Si–P bond formation nicely follows the general scheme of triplet reactivity. The ground state entrance channel of reaction (2) is rather high in energy ($\Delta H^\circ_f(P^+)+\Delta H^\circ_f(SiH_4)=325$ kcal mol^{-1}),[39] such that all $[Si, P, H_2]^+$ isomers of the triplet PES studied ($^3\mathbf{1}^+$—$^3\mathbf{4}^+$) would become accessible in terms of thermochemistry, while the expelled hydrogen molecule may remove the energy released. Notwithstanding, neither $[Si, P, H_2]^+$ nor any other $[Si, P, H_n]^+$ (n=0—4) product ions are observed in reaction (2). In fact, triplet species such as P^+ (^3P) generally prefer single bond reactions (e.g. atom abstractions and also electron transfer), while singlets can also give rise to more complex, multi-bond reactions, because these offer adequate, low-lying empty orbitals. Therefore, due to the fact that the entrance channel is quite energetic, the thermochemically allowed atom transfer reactions (2a) and (2b) effectively suppress all conceivable multi-bond pathways associated with Si–P bond formation. With respect to the recent study of Ugalde and coworkers,[22)] this finding stresses once more that purely static pictures, i.e. following the potential-energy profile, cannot predict the outcome of an ion/molecule reactions and either more sophisticated, dynamic treatments are necessary or theory has to be complemented with appropriate experimental means.

Conclusions

The $[Si, P, H_2]^{+/0}$ system exhibits rather unusual potential-energy surfaces which are in several aspects quite distinct from those of the lower homolog $[Si, N, H_2]^{+/0}$. Most strikingly, the singlet surface of the cationic system differs entirely from the nitrogen case as well as from the triplet surface of the $[Si, P, H_2]^+$ cation and that of the doublet $[Si, P, H_2]^\bullet$ radical, respectively. Thus, most of the low-energy isomers of $[Si, P, H_2]^+$ exhibit non-classical, hydrogen-bridged structures. Further, the comparison of G2 and B3LYP results, though in reasonable agreement as far as thermochemistry is concerned, reveals in several cases that the use of a mere MP2 geometry optimization in the G2 scheme is somewhat misleading. At least for the third-row elements silicon and phosphorus this approach seems to be inappropriate as far as non-classical structures are concerned. Density functional theory/Hartree–Fock hybrid methods alone can certainly not provide a solution to this issue, as these methods sometimes lead to erroneous results in unusual bonding situations which clearly outpace the desired accuracy range of a few kcal mol^{-1} (or even less) as compared to experiment. Thus, a further refinement of the G2 approach with respect to geometrical features seems to be required. In this respect, a combination of B3LYP geometries with G2-like single-point energy calculations seems to be quite promising;[40] nevertheless, a systematic survey is required to assess the validity of this approach.

The experimental studies reveal that [Si, P, H_2]$^+$ cation in its bridged form ^{1}**5**$^+$ represents a viable species to be formed in interstellar environments. But it is depleted in the presence of water due to facile formation of $SiOH^+$. Furthermore, for non-thermal ions, the formation of [Si, P, H_2]$^+$ has to compete with the efficient hydrogen transfer reaction (1c). In addition, the FTICR data demonstrate that spin is conserved in reactions of the third-row elements silicon and phosphorus; this finding is in marked contrast to the two-state reactivity observed in reactions of 3d transition-metal cations.[41]

Finally, the present study reveals that significant structural and energetic information can be gained by a combination of sophisticated theoretical and experimental means. Thus, although on practical grounds the otherwise powerful techniques[7b] such as NRMS cannot be applied for [Si, P, H_2]$^+$, the fruitful interplay of G2 and B3LYP calculations with FTICR measurements provides a quite consistent picture of the [Si, P, H_2]$^+$ potential-energy surface with regard to the relevance of these species in astrochemistry. Notably, theoretical approaches such as G2 or B3LYP alone cannot predict the outcome of a particular ion/molecule reaction, and collaboration is needed to develop a more detailed insight into product distributions.

Financial support by the Deutsche Forschungsgemeinschaft, the Volkswagen-Stiftung, the Fonds der Chemischen Industrie, and the Gesellschaft von Freunden der Technischen Universität Berlin is gratefully acknowledged. J. H. is particularly grateful for financial support from the Ministry of Education, Science, Sports and Culture, Japan, allowing his stay in IMS. Furthermore, we thank Prof. D. K. Böhme and Prof. J. M. Ugalde for providing us with preprints and Prof. S. Shaik for helpful comments.

References

1) "The Chemistry of Organic Silicon Compounds," ed by S. Patai and Z. Rappoport, Wiley, New York (1989).

2) a) The July/August 1995 issue of Chemical Reviews deals exclusively with silicon chemistry; see: J. Michl, *Chem. Rev.*, **95**, 1135 (1995); see also: b) J. M. White, *Aust. J. Chem.*, **48**, 1227 (1995).

3) For the timely controversy about the existence of the celebrated silyl ions in solution, see: L. Olsson, C.-H. Ottosson, and D. Cremer, *J. Am. Chem. Soc.*, **117**, 7460 (1995).

4) a) E. Herbst, *Angew. Chem., Int. Ed. Engl.*, **29**, 595 (1990); b) A. R. Newman, *Anal. Chem.*, **62**, 671A (1990); c) D. Smith, *Chem. Rev.*, **92**, 1473 (1992); d) see also: H. Miyoshi, K. Matsumoto, K. Kameno, H. Takaba, and T. Iwata, *Nature*, **371**, 395 (1994); e) D. Smith and P. Spanel, *Mass Spectrom. Rev.*, **14**, 255 (1996).

5) W. Kutzelnigg, *Angew. Chem.*, **96**, 262 (1984).

6) a) Y. Apeloig, in Ref. 1, p. 57; b) H. Schwarz, in Ref. 1, p. 446; c) H. Bock and B. Solouki, in Ref. 1, p. 555; d) R. Damrauer and J. A. Hankin, *Chem. Rev.*, **95**, 1137 (1995).

7) a) D. K. Böhme, "Adv. Gas Phase Ion Chemistry," JAI Press, Vol. 1, p. 225 (1992); b) N. Goldberg and H. Schwarz, submitted.

8) Additional references to silicon chemistry with elements heavier than Ne: a) K. J. Dykema, T. N. Troung, and M. S. Gordon, *J. Am. Chem. Soc.*, **107**, 4535 (1985); b) J. -G. Lee, J. E. Boggs, and A. H. Cowley, *J. Chem. Soc., Chem. Commun.*, **1985**, 773; c) T. Kudo and S. Nagase, *Organometallics*, **5**, 1207 (1986); d) B. T. Luke, J. A. Pople, M.-B. Krogh-Jespersen, Y. Apeloig, J. Chandrasekhar, and P. v. R. Schleyer, *J. Am. Chem. Soc.*, **108**, 260 (1986); e) P. D. Stout, M. W. Schmidt, P. W. Troung, and M. S. Gordon, *J. Am. Chem. Soc.*, **109**, 7644 (1987); f) H. Schnöckel and R. Köppe, *J. Am. Chem. Soc.*, **111**, 4583 (1989); g) A. Fox, S. Wlodek, A. C. Hopkinson, M. H. Lien, M. Sylvain, C. Rodriguez, and D. K. Bohme, *J. Phys. Chem.*, **93**, 1549 (1989); h) P. J. Bruna and F. Grein, *J. Phys. Chem.*, **96**, 6617 (1992); i) T. Tada and R. Yoshimura, *J. Phys. Chem.*, **97**, 1019 (1993); j) Y. Apeloig and K. Albrecht, *J. Am. Chem. Soc.*, **117**, 7263 (1995); k) R. Cipollini and F. Grandinetti, *J. Chem. Soc., Chem. Commun.*, **1995**, 773.

9) a) L. C. Snyder and Z. R. Wassermann, *Chem. Phys. Lett.*, **51**, 349 (1977); b) L. C. Snyder, Z. R. Wassermann, and J. Moskowitz, *J. Quant. Chem.*, **21**, 565 (1982).

10) H. Lischka and H. Kohler, *J. Am. Chem. Soc.*, **105**, 6646 (1983).

11) F. Kawai, T. Noro, A. Murakami, and K. Ohno, *Chem. Phys. Lett.*, **93**, 429 (1982).

12) a) J. Kachler, A. Sax, and G. Olbrich, *Int. J. Quant. Chem.*, **25**, 543 (1984); b) G. Olbrich, *Chem. Phys. Lett.*, **130**, 115 (1986); c) J. Kachler and A. Sax, *J. Chem. Phys.*, **25**, 543 (1984).

13) S. Koseki and M. S. Gordon, *J. Phys. Chem.*, **93**, 118 (1989).

14) a) K. Krogh-Joergensen, *J. Phys. Chem.*, **86**, 1492 (1982); b) K. Krogh-Joergensen, *J. Am. Chem. Soc.*, **107**, 537 (1985).

15) a) B. T. Colegrove and H. F. Schaefer, III, *J. Phys. Chem.*, **94**, 5593 (1990); b) R. S. Grev and H. F. Schaefer, III, *J. Chem. Phys.*, **97**, 7460 (1992); c) Y. Yamaguchi, B. J. DeLeeuw, C. A. Richards, Jr., H. F. Schaefer, III, and G. Frenking, *J. Am. Chem. Soc.*, **116**, 11922 (1994).

16) M. Bogey, H. Bolvin, C. Demuynck, and J. L. Destombes, *Phys. Rev. Lett.*, **66**, 413 (1991).

17) J. Hrušák, D. K. Böhme, S. Wlodek, and H. Schwarz, *J. Phys. Chem.*, **96**, 5355 (1992).

18) a) N. Goldberg, M. Iraqi, J. Hrušák, and H. Schwarz, *Int. J. Mass Spectrom. Ion Processes*, **125**, 267 (1993); b) N. Goldberg, M. Iraqi, J. Hrušák, and H. Schwarz, *J. Phys. Chem.*, **97**, 10687 (1993); c) M. C. Holthausen, D. Schröder, W. Zummack, W. Koch, and H. Schwarz, *J. Chem. Soc., Perkin Trans. 2*, **1996**, 2389; see also: d) R. Srinivas, D. Sülzle, W. Koch, C. H. DePuy, and H. Schwarz, *J. Am. Chem. Soc.*, **113**, 5970 (1991).

19) J. Hrušák and H. Schwarz, "Int. Congress on Quantum Chem.," Praha, 1994, Abstr., III-37, p. 351.

20) W. W. Schoeller and T. Busch, *J. Mol. Struct.* (*THEOCHEM*), **313**, 27 (1994).

21) For references to the rather comprehensive work of these groups, see: a) M. Essefar, A. Luna, and M. Yañez, *Chem. Phys. Lett.*, **223**, 240 (1994); b) E. M. Cruz, X. Lopez, J. M. Ugalde, and F. P. Cossio, *J. Phys. Chem.*, **99**, 6432 (1995).

22) E. M. Cruz, X. Lopez, M. Sarobe, F. P. Cossio, and J. M. Ugalde, *J. Comput. Chem.*, submitted.

23) a) L. A. Curtiss, K. Raghavachari, G. W. Trucks, and J. A. Pople, *J. Chem. Phys.*, **94**, 7221 (1991); b) K. Raghavachari and L. A. Curtiss, in "Modern Electronic Structure Theory," Part 2, ed by D. R. Yarkony, World Scientific, Singapore (1995).

24) J. A. Pople, A. P. Scott, M. W. Wong, and L. Radom, *Isr. J. Chem.*, **33**, 345 (1993).

25) A. Nicolaides and L. Radom, *J. Phys. Chem.*, **98**, 3092 (1994).

26) a) A. D. Becke, *J. Chem. Phys.*, **98**, 5648 (1993); b) P. J. Stephens, F. J. Devlin, C. F. Chabalowski, and M. J. Frisch, *J. Phys. Chem.*, **98**, 11623 (1994).

27) "Gaussian 94, Revision B.3," M. J. Frisch, G. W. Trucks, H. B. Schlegel, P. M. W. Gill, B. G. Johnson, M. A. Robb, J. R. Cheeseman, T. Keith, G. A. Petersson, J. A. Montgomery, K. Raghavachari, M. A. Al-Laham, V. G. Zakrzewski, J. V. Ortiz, J. B. Foresman, C. Y. Peng, P. Y. Ayala, W. Chen, M. W. Wong, J. L. Andres, E. S. Replogle, R. Gomperts, R. L. Martin, D. J. Fox, J. S. Binkley, D. J. DeFrees, J. Baker, J. P. Stewart, M. Head-Gordon, C. Gonzalez, and J. A. Pople, Gaussian, Inc., Pittsburgh, PA (1995).

28) a) P. M. W. Gill, B. G. Johnson, and J. A. Pople, *Chem. Phys. Lett.*, **197**, 499 (1992); b) P. M. W. Gill, B. G. Johnson, J. A. Pople, and M. J. Frisch, *J. Int. Quant. Chem. Symp.*, **26**, 319 (1992).

29) B. G. Johnson, C. A. Gonzales, and P. M. W. Gill, *Chem. Phys. Lett.*, **221**, 100 (1994).

30) C. A. Gonzales and H. B. Schlegel, *J. Phys. Chem.*, **90**, 2154 (1989).

31) "Gaussian 92, Revision F.2," M. J. Frisch, G. W. Trucks, M. Head-Gordon, P. M. W. Gill, M. W. Wong, B. G. Foresman, B. G. Johnson, H. B. Schlegel, M. A. Robb, E. S. Replogle, R. Gomperts, J. L. Anders, K. Raghavachari, J. S. Binkley, C. Gonzalez, R. L. Martin, D. J. Fox, D. J. DeFrees, J. Baker, J. J. P. Stewart, and J. A. Pople, Gaussian, Inc., Pittsburgh, PA (1993).

32) S. Cradock, E. A. V. Ebsworth, W. J. Savage, and R. A. Whiteford, *J. Chem. Soc., Faraday Trans. 2*, **68**, 934 (1972).

33) a) K. Eller and H. Schwarz, *Int. J. Mass Spectrom. Ion Processes*, **93**, 243 (1989); b) K. Eller, W. Zummack, and H. Schwarz, *J. Am. Chem. Soc.*, **112**, 621 (1990).

34) a) S. Wlodek and D. K. Bohme, *J. Am. Chem. Soc.*, **109**, 6663 (1987); b) D. Stöckigt, N. Goldberg, J. Hrušák, D. Sülzle, and H. Schwarz, *J. Am. Chem. Soc.*, **116**, 8300 (1994).

35) J. E. Bartmess and R. M. Georgiadis, *Vacuum*, **33**, 149 (1983).

36) N. Goldberg and H. Schwarz, *Acc. Chem. Res.*, **27**, 347 (1994).

37) A. Nicolaides, A. Rauk, M. N. Glukhovtsev, and L. Radom, *J. Phys. Chem.*, **100**, 17460 (1996).

38) D. Smith, B. J. McIntosh, and N. G. Adams, *J. Chem. Phys.*, **90**, 6213 (1989).

39) S. G. Lias, J. E. Bartmess, J. F. Liebman, J. L. Holmes, R. D. Levin, and W. G. Mallard, "Gas Phase Ion and Neutral Thermochemistry," *J. Phys. Chem. Ref. Data*, **17**, Suppl. 1 (1988).

40) C. W. Bauschlicher, Jr., and H. Partridge, *J. Chem. Phys.*, **103**, 1788 (1995).

41) a) A. Fiedler, D. Schröder, S. Shaik, and H. Schwarz, *J. Am. Chem. Soc.*, **116**, 10734 (1994); b) S. Shaik, D. Danovich, A. Fiedler, D. Schröder, and H. Schwarz, *Helv. Chim. Acta*, **78**, 1393 (1995).